Journal of Visualization, Vol.6, No.1 (2003) 21−29

Preliminary Study of Two Immiscible Liquid Layers Subjected to a Horizontal Temperature Gradient

Someya, S.*[1], Munakata, T.*[1], Nishio, M.*[1] and Okamoto, K.*[2]

*1 National Institute of Advanced Industrial Science and Technology, Tsukuba, Ibaraki 305-8564, Japan.
*2 Nuclear Engineering Research Laboratory, University of Tokyo, Tokai, Ibaraki 319-1188, Japan.

Received 28 May 2002
Revised 24 September 2002

Abstract : Marangoni convection, driven by interfacial instability due to a surface tension gradient, presents a significant problem in the crystal growth process. To achieve better materials processing, it is necessary to suppress and control this convection, especially in crystal growth using Liquid Encapsulated Czochralski techniques in which the melt is encapsulated in an immiscible medium. Marangoni convection can occur at the liquid-liquid interface and at the gas-liquid free surface. Buoyancy driven convection can also affect and complicate the flow. The present report studied Marangoni convection in a two-liquid layer system in an open and enclosed cavity. Flow in the cavity was subjected to a horizontal temperature gradient. Interactive flow near the liquid-liquid interface was measured by the Particle Image Velocimetry (PIV) technique. The measured flow field is in good agreement with numerical predictions.

Keywords : Visualization, Marangoni convection, Interface, Free surface, Natural convection.

1. Introduction

In order to grow single crystals of good quality for semiconductor materials, several liquid encapsulation techniques have been used in recent years. The quality of single crystals is largely affected by convection in the melt and the volatilization of ingredients. Marangoni convection often affects convective motion in the melt (especially in microgravity conditions). The driving force, the surface tension gradient, is caused by either a temperature or concentration distribution on the surface and at the interface. Liquid encapsulation techniques may offer the possibility for suppressing and controlling convective flow in the melt without the resulting vaporization loss if a liquid encapsulant with suitable physicochemical properties can be found. For example, as shown in Fig. 1(a), a liquid encapsulation technique has been applied to Czochralski (CZ) melt growth to avoid volatilization from the free surface and control natural convection at the free surface of the melt, for example, in GaAs growth. Nevertheless, there is still a free interface between the melt and the encapsulant at which natural convection can occur. In the Liquid Encapsulated Czochralski (LEC) method, convection can be driven by buoyancy and by differences in surface tension. Buoyancy-

driven convection in the encapsulant is thought to dominate the flow in the melt. Marangoni forces, however slight, may still exert an effect on the molten flow in the LEC method when crystals are grown in a 1 g environment on the ground. Such minute effects may make the flow unstable. Therefore, it is very important to understand the interaction between buoyancy-driven convection and Marangoni convection at the free surface and/or at the interface for the liquid encapsulation process of the crystal growth.

Liu et al. (1994) simulated the flow in a horizontal two-layer system subjected to a horizontal temperature gradient along the interface between two immiscible fluids. They assumed a flat interface in a zero gravity field and investigated the effects of geometrical factors and physicochemical properties. Azuma et al. (1991) conducted experimental studies about the combined effects of Marangoni and buoyancy forces in a double-layer system. They demonstrated some typical flow patterns. Jing et. al. (1997) provided a detailed discussion of the effects of the liquid depth ratio, oscillatory instability and interface contamination on the critical conditions for the incipience of thermal Rayleigh-Marangoni convection in horizontal benzene-water and water-CCl_4 two-liquid layers, based on the assumption of a flat non-deformable interface. Lopez et al. (1999) studied GaSb crystal processing by the Liquid Encapsulated Melt Zone (LEMZ) technique, shown in Fig. 1(b), in a microgravity environment and in a 1 g environment as on the ground. They characterized the properties of GaSb crystal grown by the LEMZ method and determined the effects of gravity and other processing parameters which largely influenced the final properties of crystal. However, the accuracy of measurements in these studies was not high enough. Very few papers investigate the flow field experimentally and numerically and show good agreement with the velocity field. Moreover, some reports have concluded that Marangoni convection is not observed, such as the report by Kimura et al. (1986). A number of numerical studies have been performed in which a relatively large Marangoni (Ma) number and small Rayleigh (Ra) number are assumed.

In the present paper, we carried out our experiments in a simple system with a double-liquid layer. It is very important to study this system in order to improve LEC crystal growth techniques on the ground. Therefore, we observed the flow behavior numerically and experimentally and investigated the combined effects of Marangoni and buoyancy forces on the flow in a double-layer system in which the flow was dominated by the buoyancy-driven convection.

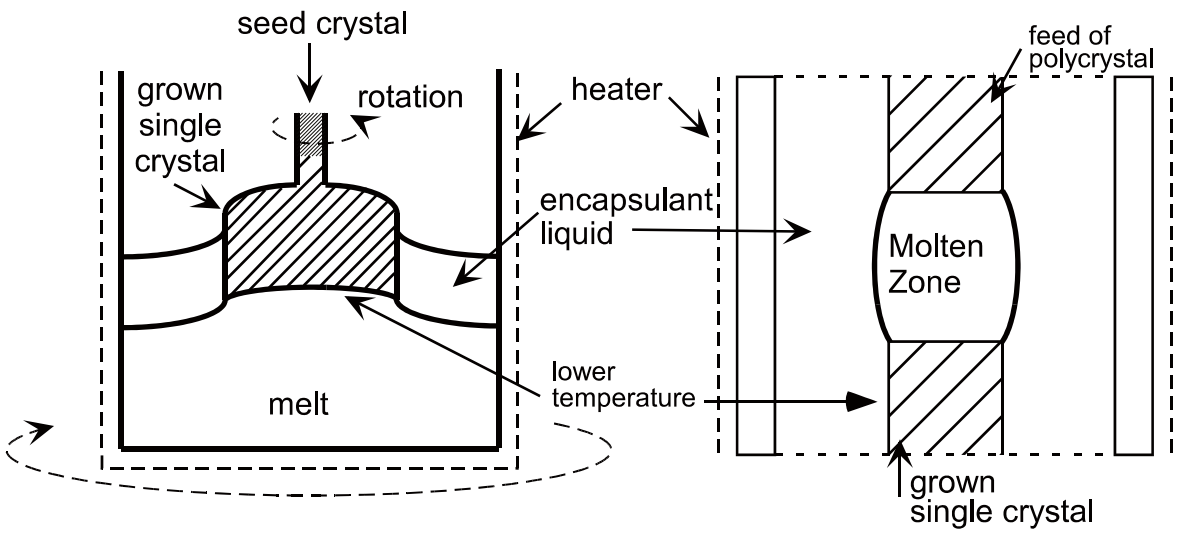

Fig. 1. Schematics of (a) LEC and (b) LEMZ(LEFZ) crystal growth techniques.

2. Numerical and Experimental Methods

2.1 Numerical procedure

The numerical simulation was carried out for the experimental system shown in Fig.2(a), consisting of two immiscible and incompressible viscous fluids in a 2-D cavity. The numerical simulation technique we used was reported previously by Munakata et al., (1986). It is thought to be accurate enough to allow a comparison of the numerical results with the empirical results in the present study. The fluid motion was governed by the 2-D Navier-Stokes equations, using the Boussinesq fluid approximations. The non-dimensionalized governing equations, Eqs.(1)-(4), were solved by the finite difference method. The subscript, i, means: i=1 for the upper layer and i=2 for the lower layer. The length was scaled by the height of the lower layer (H_2). These were discretized by the first-order central difference for the space and by the first-order up-wind difference for the convective terms. The stream function was solved by the SOR method. The grid intervals were regular and the grid number was (x, y) => (100, 50), i.e., 0.2mm/grid. The boundary conditions are summarized in Eqs.(5)-(11). The vertical heater and cooler sidewalls were maintained at constant temperatures. We assumed that the system was thermally insulated on the horizontal walls and on the top free surface. Both the free surface and the free interface were flat and non-deformable. The velocity boundary condition on the wall was the non-slip condition. Thus the values of the stream function on the walls and the free interface were zero. Temperature, horizontal velocity and the shear stress, which was induced by interfacial Marangoni forces, were assumed to be continuous at the liquid-liquid interface.

$$u_i = \frac{\partial \psi_i}{\partial y}, \quad v_i = -\frac{\partial \psi_i}{\partial x}, \quad \frac{\partial^2 \psi_i}{\partial x^2} + \frac{\partial^2 \psi_i}{\partial y^2} = \omega_i \tag{1}$$

$$\frac{\partial \omega_i}{\partial t} + u_i \frac{\partial \omega_i}{\partial x} + v_i \frac{\partial \omega_i}{\partial y} = A_i \left(\frac{\partial^2 \omega_i}{\partial x^2} + \frac{\partial^2 \omega_i}{\partial y^2} \right) - B_i \left(Ra_2 / Pr_2 \right) \left(\frac{\partial T_i}{\partial x} \right) \tag{2}$$

$$\frac{\partial T_i}{\partial t} + u_i \frac{\partial T_i}{\partial x} + v_i \frac{\partial T_i}{\partial y} = C_i / Pr_2 \left(\frac{\partial^2 T_i}{\partial x^2} + \frac{\partial^2 T_i}{\partial y^2} \right) \tag{3}$$

$$A_1 = \frac{\nu_1}{\nu_2}, \; B_1 = \frac{\beta_1}{\beta_2}, \; C_1 = \frac{\kappa_1}{\kappa_2}, \; A_2 = B_2 = C_2 = 1 \tag{4}$$

at x=0, 0≤y≤1 ; $T_2 = 0$, $\omega_2 = \frac{\partial^2 \psi_2}{\partial x^2}$, $\psi_2 = 0$ (5)

at x=0, 1≤ y ≤1+ H_1/H_2 ; $T_1 = 0$, $\omega_1 = \frac{\partial^2 \psi_1}{\partial x^2}$, $\psi_1 = 0$ (6)

at x = L/H_2, 0≤ y ≤1 ; $T_2 = 1$, $\omega_2 = \frac{\partial^2 \psi_2}{\partial x^2}$, $\psi_2 = 0$ (7)

at x = L/H_2, 1≤ y ≤1+ H_1/H_2 ; $T_1 = 1$, $\omega_1 = \frac{\partial^2 \psi_1}{\partial x^2}$, $\psi_1 = 0$ (8)

at y =0, 0< x < L/H_2 ; $\partial T_2 / \partial y = 0$, $\omega_2 = \frac{\partial^2 \psi_2}{\partial y^2}$, $\psi_2 = 0$ (9)

at y =1+H_1/H_2, 0< x < L/H_2 ; $\partial T_1/\partial y = 0$, ψ_1=0, $\omega_1 = \frac{\partial^2 \psi_1}{\partial y^2}$ (solid plate), (10)

$\omega_1 = \left(Ma_2 \mu_2 \sigma_1 / \mathrm{Pr}_2 \, \mu_1 \sigma_2 \right) \left(\partial T_1 / \partial x \right)$ (free surface),

$$\text{at } y=1,\ 0<x<L/H_2 \quad ;\ \frac{\partial T_2}{\partial y}=\frac{\lambda_1}{\lambda_2}\frac{\partial T_1}{\partial y},\ T_1=T_2,\ \psi_i=0, \tag{11}$$
$$u_1=u_2,\ \omega_2=(\mu_1/\mu_2)\omega_1-(Ma_2/\mathrm{Pr}_2)(\partial T_i/\partial x)$$

The Marangoni number and Rayleigh number for the lower layer were defined as $Ma_2=\sigma_{t2}\Delta TH_2/\mu_2\kappa_2$ and $Ra_2=g\beta_2\Delta T(H_2)^3/\nu_2\kappa_2$. Here, μ, ν, κ, β are the dynamic and kinematic viscosities, the thermal diffusivity, and the thermal expansion coefficient, respectively. "g" is the acceleration of gravity; ΔT is the temperature difference; and σ_t is the absolute value of the surface tension gradient with respect to temperature. All of the thermo-physical properties are summarized in Table 1. Pr and λ are the Prandtl number and the thermal conductivity, respectively.

Table 1. Thermo-physical properties of working fluids in numerical and experimental investigation.

	density (kg/m^3)	ν (m^2/s)	λ (W/m/K)	κ (m^2/sec)	β (1/K)	Pr	σ_t (mN/m/K)
Silicone oil KF96L-2cSt	873	2.00x10^{-6}	0.109	7.09x10^{-8}	0.00124	28.2	-0.067
Fluorinert FC-40	1870	2.20x10^{-6}	0.0670	3.38x10^{-8}	0.00120	64.3	-0.044

2.2 Experimental setup

The double-layer system with two immiscible liquids is shown schematically in Fig. 2(a). The experiments were carried out with fixed geometrical parameters, except for the existence of the removable solid top plate of bakelite. The width of the cavity, L, was 20 mm and the heights, H_1, H_2, were 5 mm each. The depth of the system was 100 mm. We assumed that the flow was 2-D and unaffected by the walls and thermal radiation from the side walls. The heater and cooler were made of copper, and the temperatures T_h and T_c were controlled by a wire heater and temperature regulator bath. The temperature difference, T_h - T_c, was maintained at 4.0[K]. The working fluids were silicone oil (KF96L-2cSt) and Fluorinert (FC-40). Their thermo-physical properties, given in Table 1, are well known and very stable. The surface tension gradient, at temperature, of the silicone oil was -0.067 × 10^{-3} N/(mK). The interfacial tension gradient, at temperature, between the silicone oil and Fluorinert was -0.044 × 10^{-3} N/(mK) (Otsubo et al., 2001).

The natural convective flow could be visualized inside the 2-D glass cavity with or without the bakelite top plate, i.e., with or without a free surface. The vertical cross-section of the system was illuminated by a light sheet of the second harmonic of a YAG laser (NewWave Research Co., Ltd.; double pulse system; maximum output energy of 25mJ/pulse). A high speed and high spatial resolution CMOS camera (1024 × 1024 pixels; Fastcam-Ultima1024; Photron, Limited.) was used to capture the images of tracer particles in the flow, i.e., 20.86 micro meters per pixel. The velocity field was calculated by using the PIV technique. The average diameter of tracer particles for PIV measurement in each layer was 10 μm for the upper layer and 4.5 μm for the lower layer. Tracer particle density was 0.8 g/cm^3 and 2.1 g/cm^3, respectively. All walls were coated with a fluorocarbon resin that was both oil- and water-repellent. This material repels especially silicone oil, thus keeping the meniscus of the interface between the silicone oil and Fluorinert small. We used a recursive PIV method (Hart, 2000). The initial interrogation window size was 16× 16 pixels, and the correct vectors were searched recursively with the smaller interrogation window. The sub-pixel analysis was based on the cross correlation with a Gaussian curve. Our measurement system was limited by the frequency of the double-pulse laser, 15Hz, while the camera could take a maximum of 1600 pictures/sec.

It was difficult to measure the velocity near the interface/free surface due to reflection at the interfaces and due to the unexpected residual meniscus at the walls.

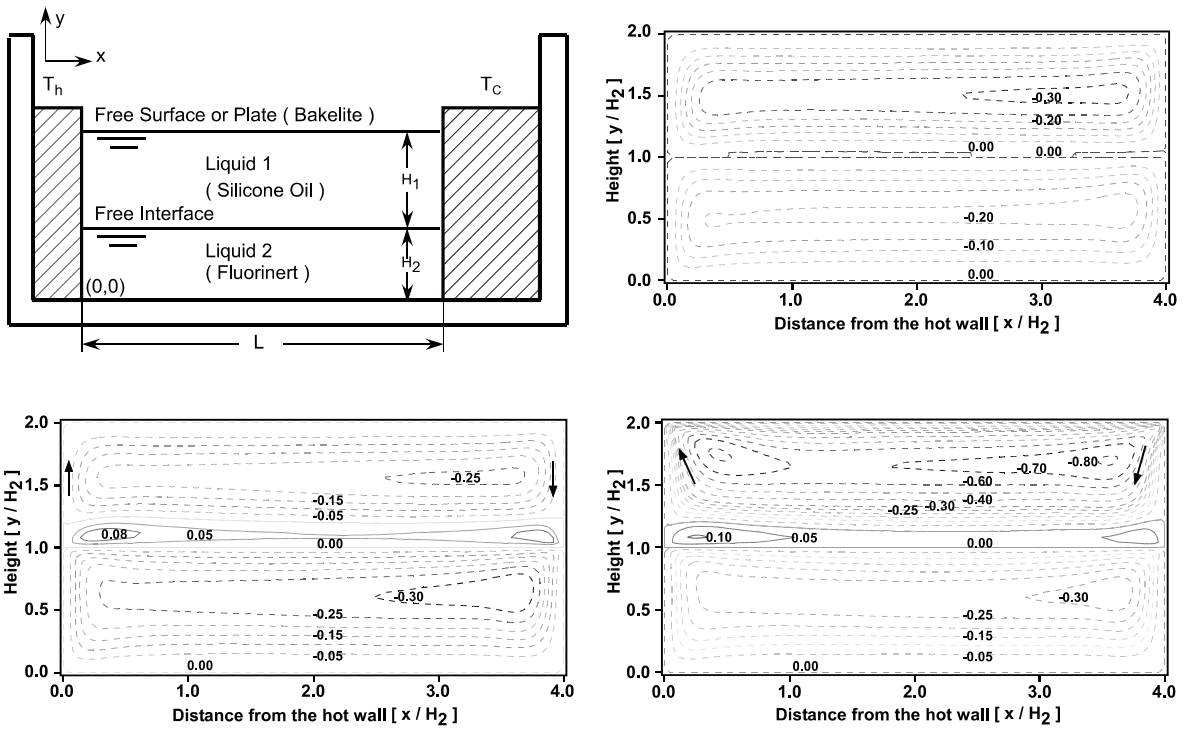

Fig. 2. (a) Schematics of the horizontal two-layered system and (b) numerical results of the flow with the covered surface and without the interfacial tension gradient, (c) with the covered surface and the interfacial tension gradient, (d) with the surface tension gradient at the free surface and the interface.

3. Results and Discussion

3.1 Numerical Results

The values of the stream function are represented by the contour lines in Figs. 2(b), 2(c) and 2(d). The intervals of the contour lines are constant (0.05), except for in a part of Fig. 2(d). Figure 2(b) shows the results obtained without Marangoni convection at the interface and with a solid top plate. In this case, Ra_1, Ra_2 and Ma_2 were 4.3×10^4, 7.8×10^4 and zero, respectively. As shown in Fig. 2(b), there was only a clockwise circulating flow in each layer. The shear stress decelerated the flow velocity near the liquid-liquid interface, and the flow became stagnant in the very narrow region just above the interface, in the upper layer of less viscous fluid. The distances between the contour lines became a little great near the liquid-liquid interface. This flow pattern is a typical buoyancy-driven flow calculated for the cavity of Fig. 2(a).

Figure 2(c) shows the numerical results of the flow field with an interfacial tension gradient and with the solid top plate. The Marangoni number in the lower layer, Ma_2, was 6.25×10^3 and the Marangoni rightward force affected the flow at the interface. Under this condition, the flow field was still dominated by buoyancy-driven convection. However, a counterclockwise vortex flow was clearly formed above the interface in Fig. 2(c), though it was not seen in Fig. 2(b) with Ma_2=0. The

counterclockwise flow was relatively strong in the region near the wall and the interface, where the local temperature gradient was relatively large. Bethancourt et al. (1999) carried out a numerical study taking the deformation of interface into consideration. They simulated a two-liquid system similar to ours for Ra=4.9 × 10^5, 2.63 × 10^7 and Ma=0, 1.6 × 10^5, 2.9 × 10^5, while they defined the horizontal width, *L*, as a reference for the non-dimensional numbers. They found that the flow became unstable when Ra and Ma were on the same order, and a counterclockwise vortex was formed in the upper layer in the region near the wall and at the interface when Ra and Ma were 2.63 × 10^7 and 2.9 × 10^5, respectively. Based on their definition, Ra and Ma in our study (Fig. 2(c)) were 5.0 × 10^6 and 2.5 × 10^4, respectively. These were smaller than (Ra=)2.63 × 10^7 and (Ma=)2.9 × 10^5 in their study. The thermo-physical properties in Table 1 were also different from those in Bethancourt's study (1999). In addition, we chose to neglect interface deformation. However, our results (Fig. 2(c)) are in agreement with Bethancourt's study (1999) with respect to the generation of a counterclockwise vortex. Thus, even in a flow field dominated by buoyancy-driven convection, the interfacial Marangoni force can affect the flow in a two-liquid-layer system. In general, even a small vortex can induce instability in the flow. It is therefore very important to understand this instability in order to control the melt flow.

In practice, the LEC and LEMZ systems have a free surface, while the encapsulant is a highly viscous melting glass. However, the free surface is in general one of the most unstable boundary conditions of flow. We are not certain about the Ra and Ma numbers in the melting glass, but there may be a surface tension gradient. Therefore, we would like to investigate the flow in the two-layer system with a free surface in order to obtain a fundamental and broad understanding of the flow in the LEC system. The results of a free surface with Marangoni convection are shown in Fig. 2(d). Ra_2 and Ma_2 were the same as in Fig. 2(c) and the Ma number on the free surface, Ma_1, was 10,823. The counterclockwise flow region in Fig. 2(d) became more narrow than that in Fig. 2(c). The flow velocity in the upper layer, especially near the free surface, became much larger than that with the covered surface. The flow pattern in the upper layer in Fig. 2(d) also changed. The upward flow toward the free surface (arrow near the hot wall) and the downward flow from the free surface (arrow near the cold wall) sloped, while these were parallel to the walls with the covered surface (arrows in Fig. 2(c)). These changes in flow pattern are thought to be due Marangoni at the free surface, although our numerical study included numerous assumptions, e.g., a flat free surface/interface and a contact angle without a meniscus.

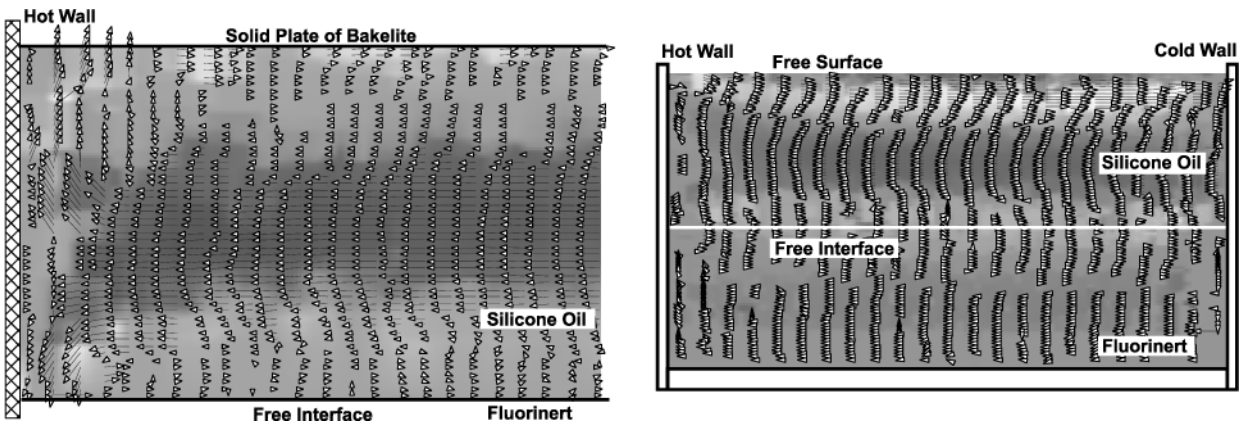

Fig. 3. Visualized flow field (a) in silicone oil layer near the hot wall with a covered surface, and (b) in 2 layers with a free surface.

3.2 Experimental Results

Empirical investigations are also very important, although taking an accurate measurement of the flow field is very difficult due to the larger spatial velocity gradient in the cavity. A reliable measurement system should be developed in order to obtain a better understanding of the flow field in the two-layer system, even under conditions of a higher Ra and Ma numbers, which are difficult to simulated numerically. We tried to measure the velocity field with PIV as accurately as possible and compared the results with numerical simulation results in an attempt to validate the measurement system.

Figure 3(a) shows the measured velocities near the hot wall in the upper layer with a solid top plate. All of the experimental conditions corresponded to the conditions in the numerical simulation shown in Fig. 2(c). The arrows show the flow direction and velocity, though it is still a little difficult to understand the velocity from the arrows in Fig. 3(a). We overlaid another map indicating the horizontal velocity. The rightward velocity is large in the white area, while the leftward velocity is large in the black area. Due to reflection at the interface and on the solid plate, and also due to the small meniscus on the glass plate in front of the camera, it was impossible to visualize the flow in the region very close to the interface. The velocities in the middle region of the cavity and near the wall were much larger than those near the interface. The large difference in velocities made it difficult to measure the flow near the interface due to the limited dynamic range of PIV measurement. However, the rightward flow just above the interface and the counterclockwise circulating flow could be observed in Fig. 3(a), although the flow velocities near the contact point between the wall and the interface were quite different from the numerical results shown in Fig. 2(c).

The measured velocity map in the whole system with a free surface is shown in Fig. 3(b). All of the experimental conditions corresponded to the conditions in the numerical simulation shown in Fig. 2(d). A rightward flow was observed near the hot wall just above the interface in this case, too. Another vortex flow near the cold wall shown in Fig. 2(d) could not be observed in this case. The meniscus at the hot/cold wall may be the cause the different flow fields in the numerical and experimental results. The direction of upward flow toward the free surface near the hot wall in Fig. 3(b) was obviously different from that in Fig. 3(a) without the free surface.

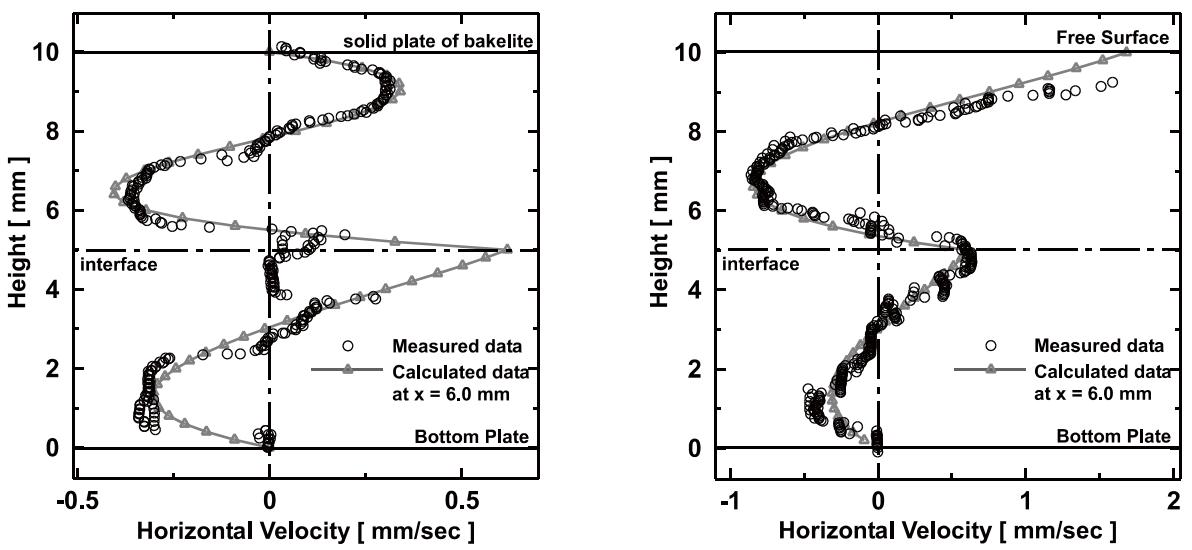

Fig. 4. Measured and calculated horizontal velocities at x=6.0mm from the hot wall, (a) with the covered surface, and (b) with the free surface.

Figures 4(a) and 4(b) summarize the horizontal components of the measured and calculated velocities along the vertical axis at 6.0 mm from the hot wall. Fig. 4(a) is the result with the solid top plate and Fig. 4(b) is the result with the free surface. As shown in Fig. 4(a), the measured velocities are in good agreement with the calculated ones except for those near the interface. The disagreement in this region may be caused by the complex and very slow flow as well as by the strong reflections at the interface. The latter was particularly noted for the case of the solid non-transparent top plate. The reflection of light at the interface was stronger with the solid plate (Fig. 4(a)) than that with the free surface (Fig. 4(b)), while the reflection at the free surface in Fig. 4(b) was more intense than that at the solid plate in Fig.4(a). The velocity near the interface was in relatively good agreement in the case of the free surface, as shown in Fig. 4(b). The velocity distribution is a little different just below the free surface in Fig. 4(b). This may be also due to introduction of the assumption of a flat free surface without a meniscus. The deformation of the surface shape and the capillary waves on the surface should be considered in the future. Also, the visualization technique and the PIV analysis still have room for improvement. However, the absolute values of the measured velocities are quite consistent with the calculated ones. It is thought that the velocity field could be measured successfully with a two-immiscible-layer system in a cavity.

4. Conclusion

The flow in two layers of immiscible liquids, with or without a free liquid-air surface, was investigated. Only in the presence of an interfacial tension gradient, a counterclockwise flow was numerically observed in the upper layer, independently of the existence of the free surface. As a preliminary step, the Ra and Ma numbers in this study were relatively small: 4.3×10^4 and 1.1×10^4 for the upper layer, 7.8×10^4 and 6.25×10^3 for the lower layer, respectively. This is the first study to observe a counterclockwise flow above the interface and to measure the flow under the condition that the flow field was dominated mainly by buoyancy-driven convection. The velocity field in the interfacial Marangoni convection was measured by the PIV technique. The measured velocities were in good agreement with the numerical results.

References

Azuma, H., Yoshihara, S., Ohnishi, M. and Doi, T., Upper Layer Flow Phenomena in Two Immiscible Liquid Layers Subject to a Horizontal Temperature Gradient, Proc. Microgravity Fluid Mechanics IUTAM Symp. Bremen, (1991), 205-212.

Bethancourt, A. M., Hashiguchi, L. M., Kuwahara, K. and Hyun, J.M., Natural Convection of a two Layer Fluid in a Side-heated Cavity, Int. J. of Heat and Mass Transfer, 42, (1999), 2427-2437.

Hart, D. P., Super-resolution PIV by Recursive Local-correlation, J. of Visualization, 3(2), (2000), 187-194.

Jing, Ch., Sato, T. and Imaishi, N., Rayleigh-Marangoni Thermal Instability in Two-liquid Layer Systems, Microgravity Science Technology, X/1, (1997), 21-28.

Kimura, T., Heya, N., Takeuchi, M. and Isomi, H., Natural Convection Heat Transfer Phenomena in an Enclosure Filled with Two Stratify Fluids, JSME(B), 52, (1986), 617-625. (*in Japanese*)

Liu Q. S. and Roux B., Marangoni Convection in Immiscible Double Liquid Layers, Microgravity Science Technology, VII/1, (1994), 103-111.

Lopez, C. R., Mileham, J. R. and Abbaschian, R., Microgravity Growth of GaSb Single Crystals by the Liquid Encapsulated Melt Zone (LEMZ) Technique, J. Crystal Growth, 200, (1999), 1-12.

Munakata, T. and Tanasawa, I., Buoyancy and Surface Tension Driven Natural Convection with Solidification, Proc. of the 8th International Heat Transfer Conference, San Francisco, U.S.A., 4, (1986), 1733-1738.

Otsubo, F., Kuwahara, K. and Doi, T., Effect of Temperature and Storage Time on the Surface Tension of the Silicone Oil and Fluorinert, J. Japan Society of Microgravity Application, 18(1), (2001), 29-34.

Author Profile

Satoshi Someya: He received his Ph. D. degree in Nuclear Engineering in 1998 from University of Tokyo, then worked as a Research Fellow of New Energy and Industrial Technology Development Organization (NEDO) (1998-2000) in the Mechanical Engineering Laboratory of AIST. He has worked in National Institute of Advanced Industrial Science and Technology (AIST) Tsukuba as a temporary researcher. He is a member of Thermal Engineering Research Group. His research interests are Crystal Growth, CO_2 sequestration, Flow Induced Vibration and Flow Visualization.

Tetsuo Munakata: He received his Ph.D. in Mechanical Engineering Department, the University of Tokyo in 1988. After completion his Ph.D. program, he has been a stuff of Mechanical Engineering Laboratory, AIST, MITI, and currently is a Group Leader of Thermal Engineering Research Group, Institute for Energy Utilization, AIST. His research interests are crystal growth, thermal phenomena under external force field and numerical simulation.

Masahiro Nishio: He received his MSc (Eng) in Chemical Engineering in 1987 from Yokohama National University. He also received Ph.D. in Chemical Engineering in 1990 from Yokohama National University, then worked as a researcher for Mechanical Engineering Laboratory, AIST, MITI. He has been working in the National Institute of Advanced Industrial Science and Technology (AIST) Tsukuba as a senior research scientist. His research interests are CO_2 sequestration technology, Crystal Growth of Gas Hydrate and Flow Visualization.

Koji Okamoto: He received his MSc (Eng) in Nuclear Engineering in 1985 from University of Tokyo. He also received his Ph.D. in Nuclear Engineering in 1992 from University of Tokyo. He worked in Department of Nuclear Engineering, Texas A&M University as a visiting associate professor in 1994. He has been working in the Nuclear Engineering Research Laboratory, University of Tokyo as an associate professor since 1993. His research interests are Quantitative Visualization, PIV, Holographic PIV, Flow Induced Vibration and Thermal-hydraulics in Nuclear Power Plant.